# GRAD CFD Software Validation

The Gas Release And Dispersion (GRAD) CFD modeling tool has been designed as a customized module based on the commercial general-purpose CFD software, PHOENICS [1]. GRAD CFD modeling software needs to be validated before it can be widely applied to industrial projects. The predictions of transient 3D distributions of flammable gas concentrations with the GRAD CFD module were validated using the comparisons with available experimental data on gas release and dispersion.

## *Validation Matrix*

The validation matrix contains the enclosed and non-enclosed geometries, the subsonic and sonic release flow rates and the releases of various gases, i.e. hydrogen, helium, etc. The validation matrix and some validation cases are described in this paper. Seven validation scenarios were selected to cover different industrial release environments and leak types. Table 2 shows the validation matrix, classified by the experiment conditions, such as leak types, release directions and domain types, etc. Seven scenarios covered the leaks from small subsonic releases to large choked releases. The validation work on the wide range of the Reynolds numbers ($50<Re<10^7$), the Mach numbers ($0 \leq Ma \leq 1$) and the Richardson numbers ($10^{-5}<Ri<10^4$) helped validate and calibrate the CFD models and find the suitable settings for the coefficients used in the boundary conditions and the turbulence models for the GRAD modeling.

Table 2. GRAD CFD module validation scenarios

| Case No. | Case name | Description of experiment | | | | CFD Model | Data source reference |
|---|---|---|---|---|---|---|---|
| | | Domain | Leak direction | Leak type | Experimental data | | |
| 1 | Helium jet | Open | Vertical | Subsonic, helium release | Steady-state, velocities, concentrations and turbulence intensities | Incompressible, steady-state | Reference [2] |
| 2 | $H_2$ jet | | Horizontal | Subsonic, $H_2$ release | Transient, concentrations | Incompressible, transient | Reference [3] |
| 3 | INERIS Jet | | | Choked, $H_2$ release | Steady-state, concentrations | Compressible, steady-state | Reference [4] |
| 4 | Hallway End | Semi-enclosed | Vertical | Subsonic, $H_2$ release | Transient, concentrations | Incompressible, transient and steady-state | Reference [5] |
| 5 | Hallway middle | | | Subsonic, helium release | Transient, concentrations | | |
| 6 | Garage with a car | | | Subsonic, $H_2$ and helium releases | Transient, concentrations | | Reference [6] |

| | | | | | | | |
|---|---|---|---|---|---|---|---|
| 7 | $H_2$ vessel | Enclosed | | Subsonic, $H_2$ release and dispersion | Transient, concentrations during dispersion | Incompressible, transient | Reference [7] |

Below are examples of model validation work conducted by the team within the last 5 years.

## *Hydrogen Subsonic Release in a Hallway*

An example of GRAD CFD validation work was described in detail in the earlier paper [8]. This work was conducted by AVT group while at SESC using the experimental and numerical data [5] published by Dr. M.R. Swain et al. Below is a brief description of this validation work.

A hydrogen release benchmark problem with a simple geometry was used for CFD model validation in this case. In particular, in this scenario (see Figure 1), the hydrogen was released at the rate of 2 SCFM (standard cubic feet per minute) from the floor at the left end of a hallway with the dimension of 114 in × 29 in × 48 in (2.9 m × 0.74 m ×1.22 m). At the right end of the hallway, there were a roof vent and a lower door vent for the gas ventilation. Four sensors were placed in the domain to record the local hydrogen concentration variations with time. Figure 1 shows the geometry and the numerical results obtained, i.e. the 3% hydrogen volume concentration iso-surface at 1 minute after the start of hydrogen release. The initial grid used was a coarse grid of 36×10×18 cells. It can be seen that the two different CFD codes gave very similar results. Figure 2 shows the concentrations at the four sensors obtained in [5] from numerical simulations using FLUENT and from experiments (left) and those obtained by Stuart Energy using PHOENICS. The concentration differences between the two models are about 20% for sensors 1 and 2 and 10% for sensors 3 and 4. The differences may be attributed to differences in the turbulence models, grid sensitivity, and/or the settings of boundary conditions at the inlet and the outlets (two vents).

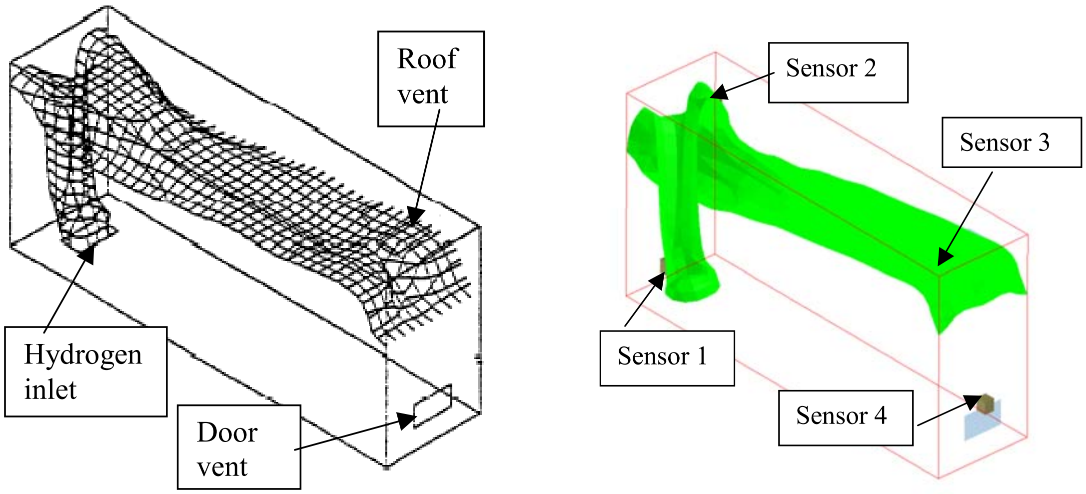


Figure 1. Comparison of concentration iso-surfaces for 2 SCFM hydrogen leak, 1 min elapsed and 3% concentration iso-surface. (Left: published data [5]; right: AVT's modeling).

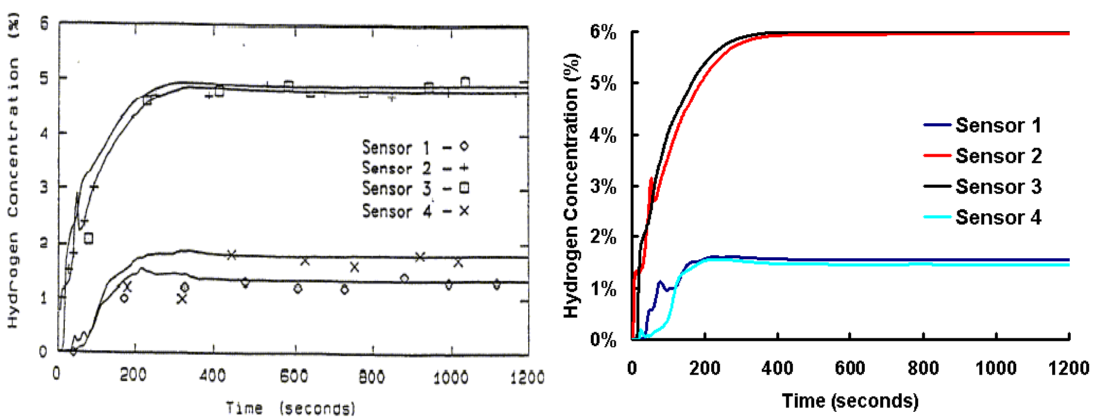


Figure 2. Comparison of concentrations at four sensors for 2 SCFM hydrogen leak and 20 minute duration. (Left: published data [5]; right: AVT's modeling).

## *Helium Subsonic Release in a Garage With a Car*

Another GRAD CFD module validation work was conducted using the experimental and numerical data published by Dr. M.R. Swain et al. [6] on the helium subsonic release in a garage with a car. Figure 2 shows the geometry of the case considered. The four small cubes mark the locations of four helium sensors in the domain.

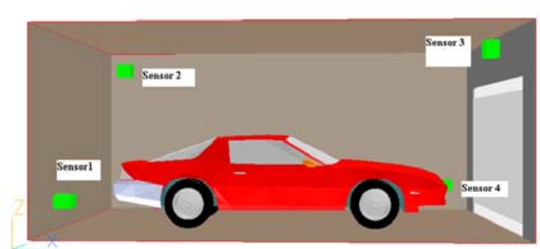


Figure 3. Geometry and helium sensors for helium subsonic release in a garage.

Local Adaptive Grid Refinement (LAGR) was also applied to this modeling case. Table 3 shows that LAGR helps reduce the predicted concentrations at the locations of Sensor 1 and Sensor 4 significantly. The predicted results are in accord with the CFD simulations reported elsewhere.

Table 3. Steady-state results for helium release in a garage with a car (LVEL turbulence model)

| Simulations | Sensor 1 | Sensor 2 | Sensor 3 | Sensor 4 |
|---|---|---|---|---|
| Swain's experimental results | 0.5% | 2.55% | 2.55% | 1.0% |
| Initial coarse grid, 32×16×16 | 1.92% | 2.53% | 2.52% | 1.94% |
| Adaptive refined, 39×26×24 | 0.98% | 2.66% | 2.62% | 1.08% |
| Adaptive refined, 58×26×27 | 0.79% | 2.70% | 2.67% | 1.01% |

## Helium Turbulent Subsonic Jet

Another example of GRAD CFD module validation work was described in the reference paper [9]. Below is the brief description of the major findings. In this validation work, a vertical helium jet reported by Panchapakesan and Lumley [2] was simulated using the GRAD CFD module. The real geometry was simplified by a 2D axi-symmetric computational domain to save the computational resources. The mixed gas was assumed to have incompressible gas properties so the inverse linear function was used to calculate the mixture density dependent on the local helium mass concentration and the helium and air densities. The $k$-$\varepsilon$ RNG turbulence model was used while solving the governing equations to predict the velocity and mass/volumetric concentration profiles. The numerical results showed a good agreement with experimental data in both radial and axial directions with the errors less than 10%. The simulation results were also compared with other published helium experimental data obtained by Keagy and Weller, Way and Libby, Aihara et al. and the correlations made by Chen and Rodi [10] for velocity and concentration. The satisfactory agreement (within 10%) between the experimental and numerical data in the three jet regions proved that the GRAD CFD model is robust, accurate and reliable, and that the CFD technique can be used as an alternative to the experiments with similar helium jets. It also indicated that the CFD model can accurately predict similar hydrogen releases and dispersion if the model is properly calibrated with hydrogen coefficients when applying to hydrogen jets. Table 4 shows the axial volumetric concentrations and axial velocities ($U_s$), along the jet centre line, obtained by the experiment [2] and current CFD simulations. The corresponding errors are shown in percentage. As we see, the $k$-$\varepsilon$ RNG model successfully predicts the concentration and velocity fields in the turbulent jet flow.

Table 4. Axial mean values of volumetric concentrations and velocities along the jet centre line

| $r = 0$ | Volumetric concentration | | | Velocity, $U_s$ | | |
|---|---|---|---|---|---|---|
| $x$ (m) | Exp. (%) | CFD (%) | Error (%) | Exp. (m/s) | CFD (m/s) | Error (%) |
| 0.306 | 18.0 | 19.3 | 7.51 | 3.15 | 3.36 | 6.67 |
| 0.3672 | 14.7 | 15.9 | 8.15 | 2.59 | 2.72 | 5.02 |

| | | | | | | |
|---|---|---|---|---|---|---|
| 0.4284 | 12.6 | 13.4 | 6.04 | 2.27 | 2.30 | 1.32 |
| 0.4896 | 11.3 | 11.5 | 2.36 | 2.01 | 2.00 | -0.50 |
| 0.5508 | 10.0 | 10.1 | 0.53 | 1.86 | 1.78 | -4.30 |
| 0.612 | 9.02 | 8.91 | -1.26 | 1.69 | 1.61 | -4.73 |
| 0.6732 | 8.30 | 7.94 | -4.09 | 1.58 | 1.48 | -6.33 |
| 0.7344 | 7.68 | 7.16 | -6.63 | 1.49 | 1.38 | -7.38 |

## *High Pressure Vertical Turbulent Natural Gas Jet*

The nature of the concentration field produced by subsonic, momentum dominated incompressible turbulent free jets is well documented in the literature. The purpose of this research effort was to validate and improve the CFD modeling of natural gas releases and dispersion by using the published experimental data obtained by Birch etc. al. [1984 and 1987] for high pressure vertical turbulent natural gas release. The approach is to compare the concentration fields along the center line predicted by CFD simulations to the empirical data. The validating pressures for the natural gas releases range from 3.5 bars to 71 bars, covering most applicable working conditions in industry. To provide a comprehensive database for much higher pressure, natural gas releases from more than 100 bars were also simulated, presented and compared with the correlation equation extrapolated from Birch's experimental data.

Gas releases in the form of turbulent jets and plumes rapidly achieve self-similarity, and in this similar region the flow exhibits little memory of its initial structure [A. D. Birch et al, 1984]. The distance taken for the mean volumetric concentration to decay to a given value in a momentum dominated turbulent free jet is proportional to the diameter of the source and inversely proportional to the square root of the density of the jet fluid, but is independent of jet velocity. The axial volume fraction concentration, $\overline{\eta}$, can be expressed by the axial decay constant, *k*, the downstream distance, *z*, the leak orifice, *d*, the virtual orifice displacement, *a*, density of air and gas, $\rho_a$ and $\rho_g$, and the absolute pressure of gas over the ambient pressure, $P/P_a$ [Birch 1984]:

$$\overline{\eta} = \frac{kd}{z+a}(0.582C_D\frac{P}{p_a})^{\frac{1}{2}}(\frac{\rho_a}{\rho_g})^{\frac{1}{2}}.$$

Here $C_D$ is the discharge coefficient, which is about 0.85 for 3.5 bar natural gas jet.

Figure 4 shows the non-dimensional correlation derived from the experimental data obtained by Birch for vertical turbulent natural gas jets leaking with stagnation pressure from 3.5 to 71 bars:

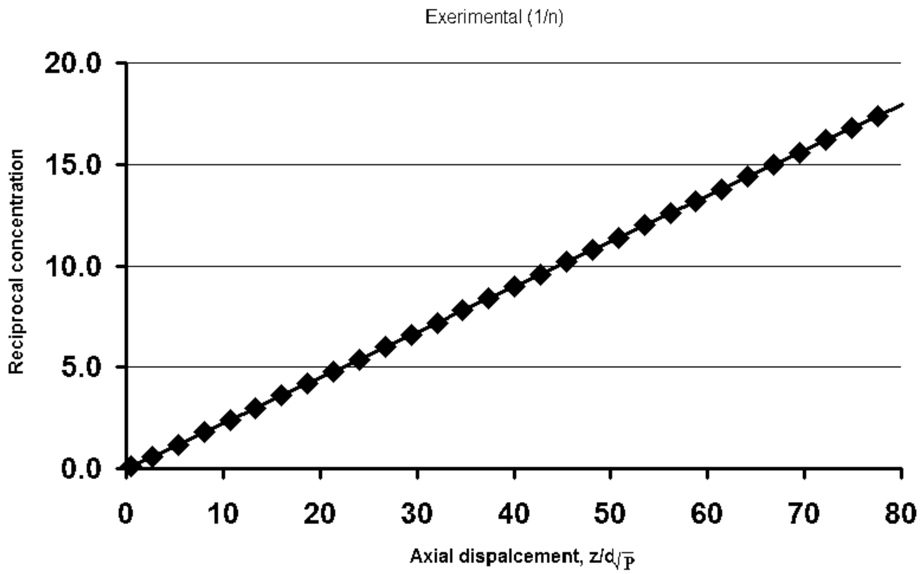


Figure 4. Reciprocal plot of mean concentration for all the high pressure natural gas results showing collapse of the data in terms of $z/d\sqrt{P}$. [A. D. Birch et al., 1984]

Birch's experiments on natural gas jets were numerically simulated by using the CFD model for methane releases and dispersion. The thermodynamic gas properties were adjusted to reflecting those of the natural gas used in the birch's experiments, that is, 92% to 92.4% of methane and a mean molecular weight of 17.32. The internal diameter of the nozzle (leak orifice) is 2.7 mm. Different symmetric domain sizes were used for the simulations. Figure 5 shows the volumetric concentrations obtained by the k-e RNG and LVEL turbulence models for 3.5 bars. The LVEL turbulence model yields the simulation results deviating from the experiment data by 50% at high NG concentrations and within 10% for lower (LFL range) concentrations while the k-e RNG model yields the results within 10% difference from the experimental within the whole concentration range. It can be seen that the CFD models for methane releases and dispersion reproduces the experimental data within the LFL range with acceptable accuracy by both turbulence models: k-e RNG gives out a very accurate CFD results although it requires a relatively large computational resources while LVEL gives out an acceptable and reliable results but it uses much less computational time and memory.

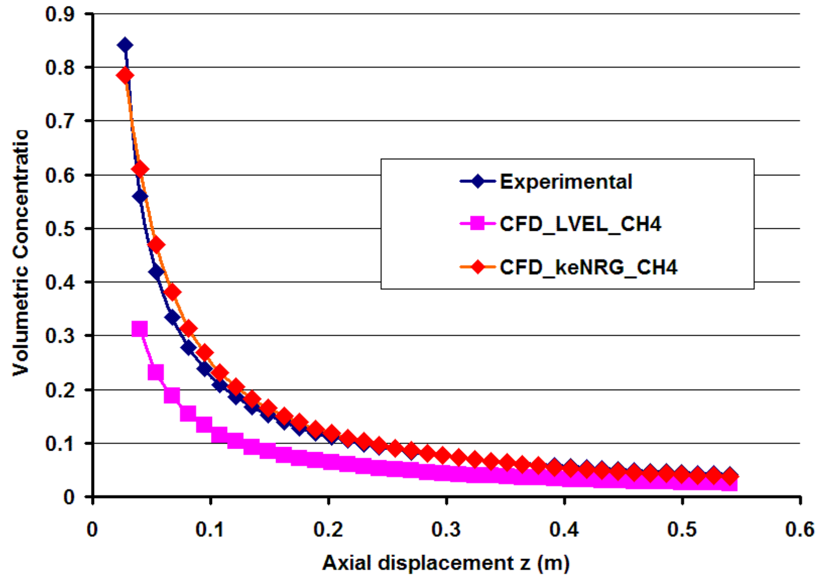


Figure 5. Comparison of CFD results with the experimental data for the decay of axial volumetric concentration with the displacement from the orifice with a pressure of 3.5 bars.

Simulations were further performed for higher pressures up to 170 bars using K-e RNG models. The natural gas turbulent diffusivity is assumed to 0.7 of turbulent viscosity, which is calculated by the kinetic energy and turbulent energy dissipation rate (k-e). Figure 6 shows the simulation data versus the experimental correlations for the pressures from 3.5 to 170 bars.

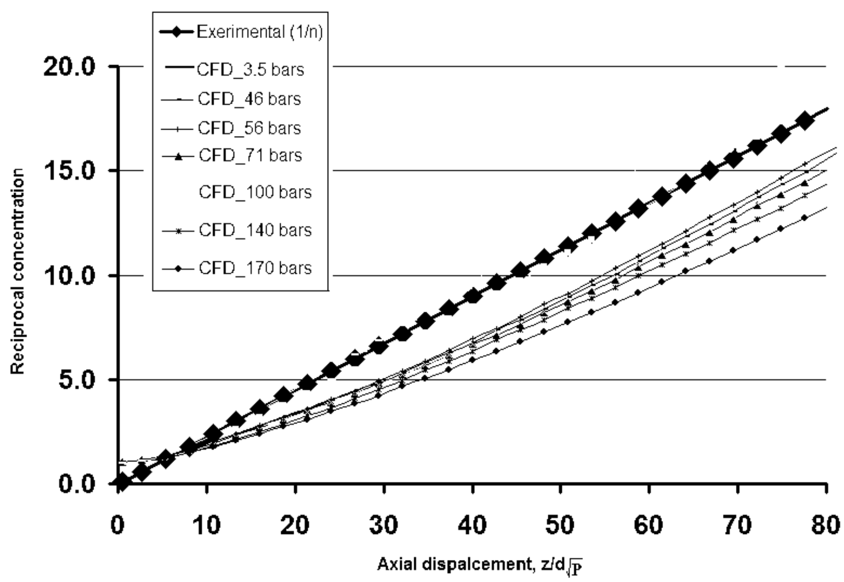


Figure 6. Comparison of CFD results with the experimental mean concentration for all the high pressure natural gas results showing collapse of the data in terms of $z/d\sqrt{P}$. Pressure range: 3.5 bars to 170 bars.

It can be seen that the numerical simulations reproduce the experimental data for various pressure with acceptable errors using the current CFD models. The errors are less than 20% for a wide range of pressures, indicating that the CFD models for the natural gas releases and dispersion can be successfully applied to the safety analysis by the prediction of mean volumetric concentration caused by the catastrophic releases.

## *INERIS Hydrogen Jet*

This example includes a validation of the compressible model developed by A.V. Tchouvelev & Associates Inc. using the experimental results obtained by Institut National de l'Environnement Industriel et des Risques (INERIS) for the leak of hydrogen from a pressurized vessel [11].

INERIS performed an experimental investigation of the concentration field of supercritical jets of hydrogen. The concentration measurements were made in the subsonic zone of the jets using catalytic fast response gas sensors that could measure the concentration of combustible gas in highly reactive environments with no risk of ignition. INERIS also measured the concentration field which resulted from the leak of hydrogen gas in free air, through a circular orifice (diameter: 0.5 mm) and coming out from a 19 litre vessel, for a storage pressure between 50 and 400 bar [11]. The experiments were designed on a large scale typical of that encountered in industry during accidental discharges of pressurized gas.

The experiments that were considered consisted of variation of pressure of the vessel from 50 bars to 400 bars while maintaining a constant orifice diameter of 0.5 mm.

The model used in PHOENICS consisted of applying appropriate boundary conditions that represent critical flow through the orifice, corresponding to the appropriate vessel pressure. The parameters at the orifice were kept constant throughout the dispersion, which represented steady state conditions. The entire vessel was not modeled so as to reduce the computational cost. The ideal gas law was used to relate the parameters at the orifice. Isothermal dispersion was modeled; therefore the critical density was adjusted based on the mass flux.

It was found that the PHOENICS model using steady state analysis overestimated the volume concentrations obtained from the INERIS results for all of the vessel pressures used. The errors between the experimental and PHOENICS results were largest for 50 bars, and the errors decreased as the pressure increased with the lowest error for 300 – 400 bars. This can be seen in Figure 7 to Figure 11.

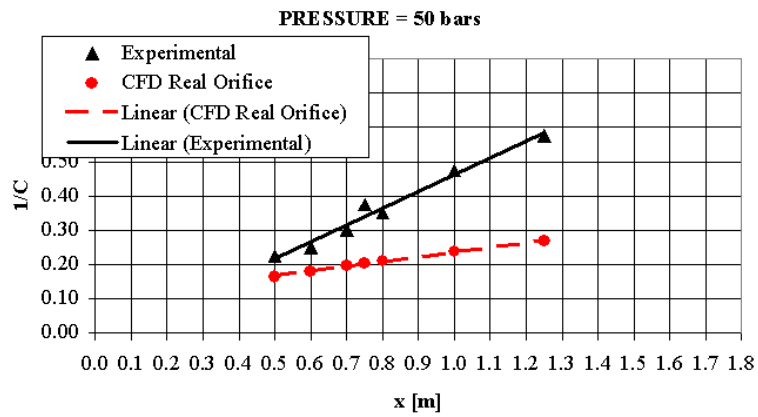


Figure 7. Pressure = 50 bars, Diameter = 0.5 mm

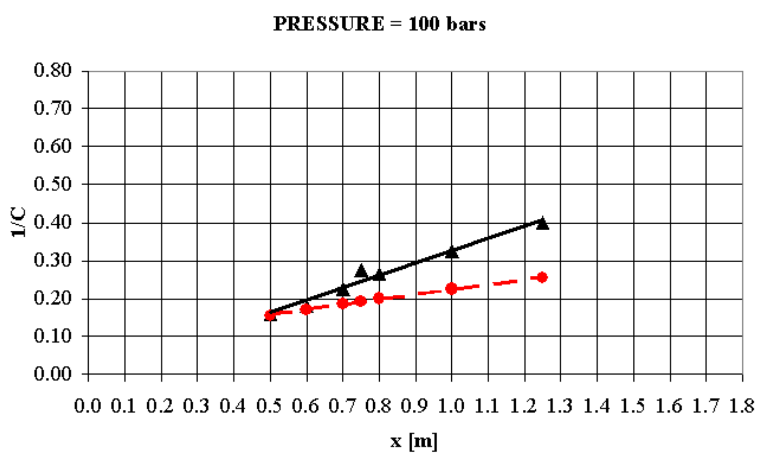


Figure 8. Pressure = 100 bars, Diameter = 0.5 mm

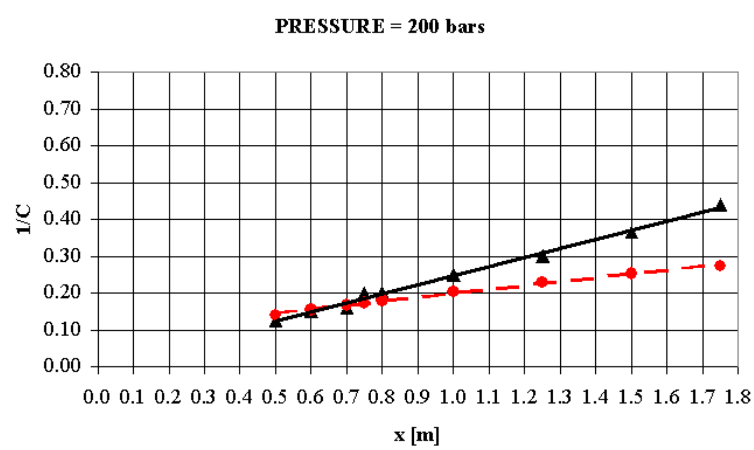


Figure 9. Pressure = 200 bars, Diameter = 0.5 mm

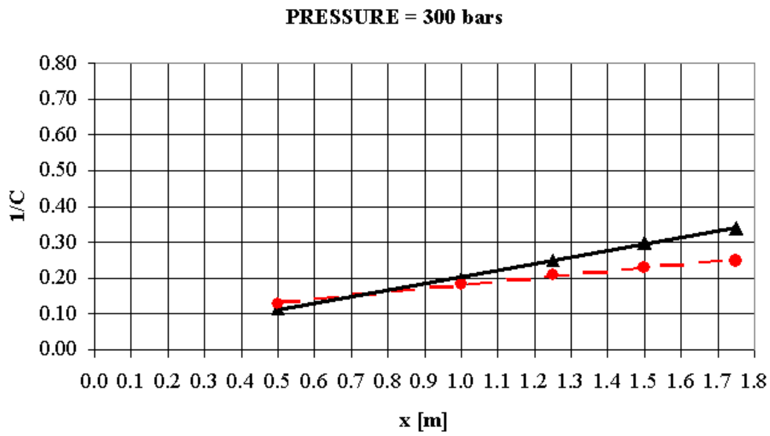


Figure 10. Pressure = 300 bars, Diameter = 0.5 mm

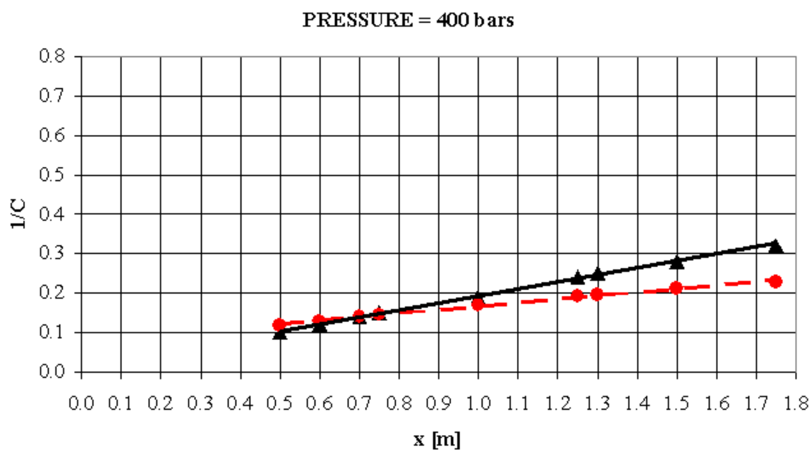


Figure 11. Pressure = 400 bars, Diameter = 0.5 mm

## References


1. PHOENICS Hard-copy Documentation (Version 3.5), Concentration, Heat and Momentum Limited, London, UK (September 2002).
2. N.R. Panchapakesan, and J.L. Lumley, Turbulence measurements in axisymmetric jets of air and helium. Part 2. Helium jet, *J. Fluid Mech*. Vol. 246, pp. 225-247 (1993).
3. M. R. Swain, Hydrogen Properties Testing and Verification (June 17, 2004).
4. E. Ruffin, Y. Mouilleau, and J. Chaineaux, Large scale characterisation of the concentration field to supercritical jets of hydrogen and methane, *J. Loss Prev. Process Industry*, vol. 9 (4), pp. 279-284 (1996).
5. M.R. Swain, E.S. Grilliot, and M.N. Swain, Risks incurred by hydrogen escaping from containers and conduits. NREL/CP-570-25315, *Proceedings of the 1998 U.S. DOE Hydrogen Program Review*.
6. M.R. Swain, J.A. Schriber, and M.N. Swain, Addendum to hydrogen vehicle safety report: residential garage safety assessment. Part II: risks in indoor vehicle storage final report.
7. Y.N. Shebeko, V.D. Keller, O.Y. Yeremenko, I.M. Smolin, M.A. Serkin, and A.Y. Korolchenko, Regularities of formation and combustion of local hydrogen-air mixtures in a large volume, *Chemical Industry*, Vol. 21, pp. 24 (728)-27 (731) (1988) (in Russian).
8. V. Agranat, Z. Cheng, and A. Tchouvelev, CFD modeling of hydrogen releases and dispersion in hydrogen energy station, *Proceeding of the 15th World Hydrogen Energy Conference*, Yokohama, Japan (June 2004).
9. Z. Cheng, V.M. Agranat, and A.V. Tchouvelev, Vertical turbulent buoyant helium jet - CFD modeling and validation, *Proceeding of the 1st International Conference on Hydrogen Safety*, Pisa, Italy (September 2005).
10. C.J. Chen, and W. Rodi, Vertical Turbulent Buoyant Jets – A review of Experimental Data, in: *The Science and Application of Heat and Mass Transfer* (Pergamon Press, 1980).
11. Chaineaux (J.), "Leak of hydrogen from a pressurized vessel. Measurement of the resulting concentration field". Workshop on dissemination of goals, preliminary results and validation of methodology, Bruxelles, 11 mars 1999, p. 156-161.